CNRS

Centre National de la Recherche Scientifique

INFN

Istituto Nazionale di Fisica Nucleare

Advanced Virgo suspension: study of the back up solution

VIR-0316D-16

Issue: 4

Date: July 13, 2016

Authors:

G. Guidi[1], P. Puppo[2]

[1]INFN, Firenze-Urbino

[2]INFN, Sezione di Roma

Abstract

After the several suspension failures on the NI and WI payloads, we have made and evaluation of the sensitivity (early, with input power of P=25W and without SR) of Advanced Virgo for the scenarios in which the mirrors are suspended with steel wires or with more robust, thicker silica fibers.

1 The optimized silica wires.

In the optimized configuration the silica fiber profiles are shaped with the aim to:

- Cancel the thermoelastic losses so that the wire losses are minimal at the pendulum frequency;
- Have the frequency of the fiber bouncing mode below 10 Hz, outside the sensitivity bandwidth;
- Have the frequency of the $theta_x$ mode (pitch) lower 1.5 Hz.
- Keep the violin modes frequency above 400 Hz, outside the control bandwith;

In this scheme, the fibers, pulled starting from a rod of 3 mm diameter, have two tapered neck sections decreasing in diameter to the 800 μm, then most of the fiber length has a diameter of 400 μm, thus setting the bouncing and violin frequencies at values suitable for the AdV purposes.

The thermal noise of the monolithic suspension of 5.8 10^{-23} $1/Hz^{1/2}$, where the upper clamping part is not negligible and is included (n.b. the optical noise is 1.5 10^{-22} $1/Hz^{1/2}$).

1 Temporary solution: the steel wires

To allow the north arm commissioning activity to start, we have suspended the NI mirror with the C85 steel having a diameter of 0.6 mm. The NE mirror is suspended with optimized silica wires.

The NI suspension set up is not optimized for a steel wire so we expect a loss angle of the order of 10^{-3} or worst. However, an optimized set up could give a loss angle not better than 10^{-4}. Moreover, in the steel material the thermoelastic loss angle is not cancelled by a proper choice of the diameter like in silica. For this reason the choice of the wire diameter can determine just the wire strength and the frequencies.

1.1 0.3mm

In Virgo the wire diameter was 0.2 mm giving a load stress in the wire of 1.6 GPa.

So, in principle this solution can be adopted, even if the design of the monolithic suspension must be checked to see if it can be adapted for this wire diameter.

In the case of a 0.3mm diameter for AdV the load stress is 1.4 GPa, the first violin is at about 310 Hz and the bouncing mode at 8 Hz

The thermal noise at 10 Hz is foreseen to be 8.06 10^{-22} $1/Hz^{1/2}$ with the steel wires of 0.3 mm diameter (optimized configuration, i.e. $\phi_{steel}=10^{-4}$, viscous Q of the marionette of 30000). In this case the thermal noise of the upper clamping system is negligible. The estimation of the ranges is given in the Table 1.

1.2 0.4mm

We also analyze the configuration of 0.4 mm diameter which can be easier to be used to the Advanced Virgo mirrors suspension system, not designed for using steel wires.

In the case of a 0.4mm diameter for AdV the load stress is 0.8 GPa, the first violin is at about 310 Hz and the bouncing mode at 8 Hz

The thermal noise at 10 Hz is foreseen to be 8.06 10^{-22} $1/Hz^{1/2}$ with the steel wires of 0.3 mm diameter (optimized configuration, i.e. $\phi_{steel}=10^{-4}$, viscous Q of the marionette of 30000). In this case the thermal noise of the upper clamping system is negligible. The estimation of the ranges is given in the Table 1.

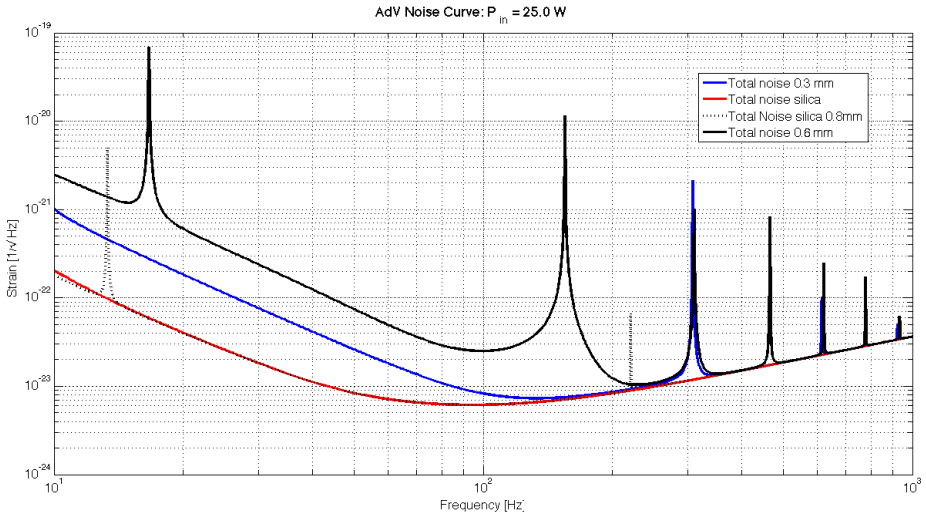

Figure 1: Comparison between the sensitivities (early) for four different cases: Official (red), Silica wires with 0.8mm diameter (black dotted), steel wires with diameter 0.3 (blue) and loss angle 10^{-4}, steel wires with diameter 0.6 (blue) and loss angle 10^{-3} (black).

	Silica opt	***Steel 400 µm***	Steel 300 µm	***Silica 800 µm***	Steel 600 µm, ϕ=1e-3 (ϕ=1e-4)	VirgoPlus 250 µm silica wires
Violin (Hz)	**440**	***231***	307	***220***	155	430
Bouncing	**8.0**	***11.1***	8.3	***13.3***	16	15
BNS Range (Mpc)	**109.9**	***45.4***	61	***109.8***	21 (25)	46
BBH Range (Mpc)	**1023**	***202***	315	***1026***	83 (109)	393
Stochastic	**5.7 10^{-9}**	***2.1 10^{-7}***	8.4 10^{-8}	***5.8 10^{-9}***	1.4 10^{-6}	1.9 10^{-8}

Table 1: Evaluation of the ranges, for 4 payloads, using the gwinc version used for the computation of the official sensitivities curves. For comparison the VirgoPlus numbers are shown.

1.3 0.6mm

In the case of a 0.6mm diameter, the first violin is at about 155 Hz and the bouncing mode at 16 Hz

The thermal noise at 10 Hz is foreseen to be 4.2 10^{-21} $1/Hz^{1/2}$ with the steel wires of 0.6 mm diameter (not optimized configuration, i.e. $\phi_{steel}=10^{-3}$, viscous Q of the marionette of 30000). In this case the thermal noise of the upper clamping system is negligible. The estimation of the ranges is given in the Table 1.

2 Silica wires with 0.8mm diameter

Another backup solution can be the use of enforced silica wires having a cylindrical shape and a diameter of 0.8 mm. In this case the suspension is safer and the sensitivity can be preserved.

In this case the sensitivity does not change as the thermal noise depends on the thicker portion of the fiber which keeps the diameter of 0.8mm. (see Figure 1)

The change is on the lower violin frequency of 220 Hz and the bouncing mode at 13.3 Hz.

We notice that although the bouncing mode is greater, the pitch mode, important for the control activity, should remain similar to the optimized silica solution as it depend on the bending zone of the wire which is still 0.8mm. The estimation of the ranges is given in the Table 1.

2 Case of only one mirror suspended with steel wire

We have made an evaluation of the sensitivities in the case only one suspension is done with steel. In this case two types of violin modes are present in the bandwidth. The ranges are shown in the Table 2

	Silica opt	***Steel 400 µm***	Steel 300 µm
Violin (Hz)	**440**	***231***	307
Bouncing	**8.0**	***11.1***	8.3
BNS Range (Mpc)	**109.9**	***65***	80
BBH Range (Mpc)	**1023**	***379***	548
Stochastic	**$5.7\ 10^{-9}$**	***$2.1\ 10^{-7}$***	$2.8\ 10^{-8}$

Table 2: Ranges in the case only one suspension is made of steel.

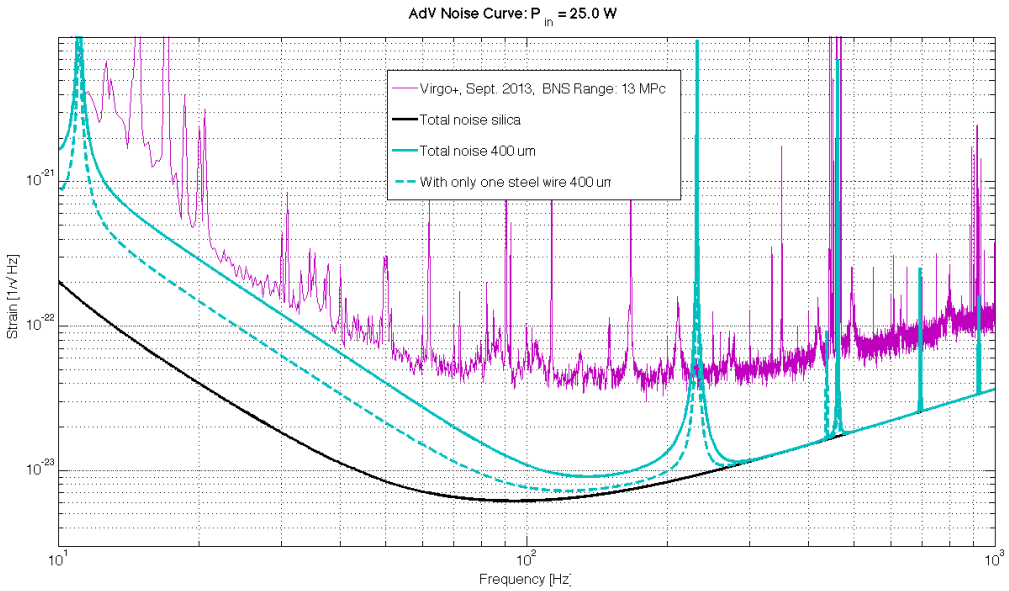

Figure 2: Green curve refers to 4 steel suspensions with 0.4mm diameter (phi=1e-4), the dotted green curve refers to 1 steel suspension (0.4mm and loss angle=10^{-4}) and 4 suspensions of fused silica. They are all compared with the official sensitivity (black curve).

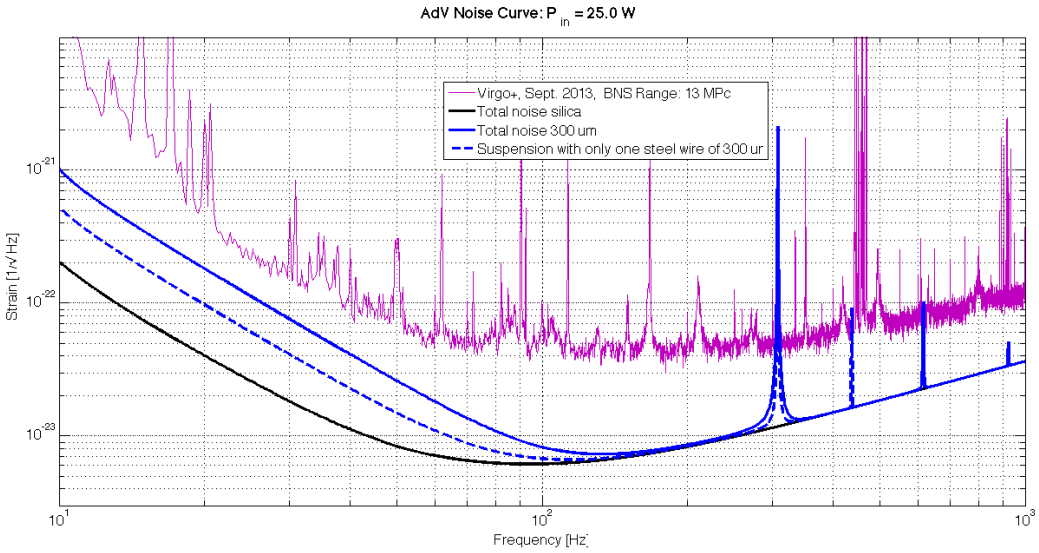

Figure 3: Blue curve refers to 4 steel suspensions with 0.3mm diameter (phi=1e-4), the dotted blue curve refers to 1 steel suspension (0.3mm phi=10^{-4}) and 4 suspensions of fused silica. They are all compared with the official sensitivity (black curve).

3 Evaluation with the new gwinc version of the case 2 silica +2 steel suspensions.

We have calculated the ranges in the case 2 suspensions are with steel wires and the other ones are in silica. This will be probably the starting configuration for Virgo Advanced that will lead to the scientific run with Ligo O2.

	Silica opt	***Steel 400 μm (ϕ=10^{-4}) (ϕ=10^{-3})***	Steel 300 μm (ϕ=10^{-4}) (ϕ=10^{-3})	Steel 600 μm (ϕ=10^{-3})(1 steel 0.3mm, 1 steel 0.6mm, 2 silica wires)
Violin (Hz)	**440**	***231***	307	
Bouncing	**8.0**	***11.1***	8.3	
BNS Range (Mpc)	**105.5**	***54 (46)***	69(59)	27(32)
BBH Range (Mpc)	**979**	***279(195)***	419(274)	117(159)

Table 3:Ranges for different suspension setup in which 2 suspensions are with fused silica fibers and other 2 with steel wires. The 600μm column contains also an estimation of the range supposing that one suspension is 300 μm with loss angle 10^{-4} and the other one is 600 μm with loss angle 10^{-3}.

The calculation of the ranges were performed using a new version of the gwinc, a bit different from the one used to compute the official curve.

The differences between the gwinc previously used are:

- Coating Brownian Noise based on experimental measurements performed at LMA by M. Granata (see (VIR-0204A-15) note).
- The gravity gradient noise is based on the on site measurements of the ground seismic noise performed by Irene Fiori.

We have spanned some different configurations (see Table 3) both for the steel wired diameters and for the loss angles. In the Figure 4 and Figure 5 the sensitivities for the worst and the optimal configuration are compared.

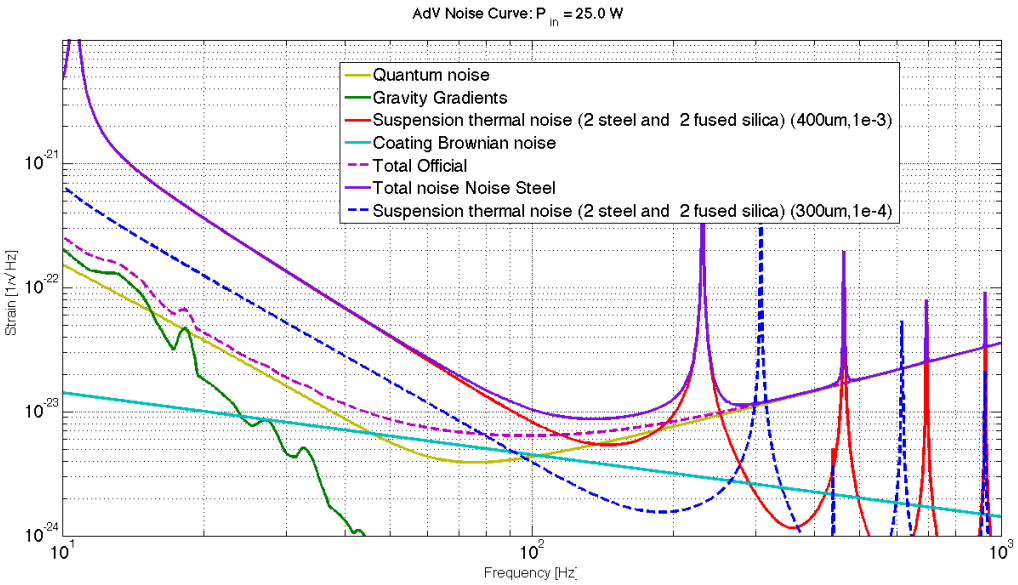

1. **Figure 4: Sensitivities for two silica+ two steel wired payloads. The dimensions of the wire is shown in the legends.**

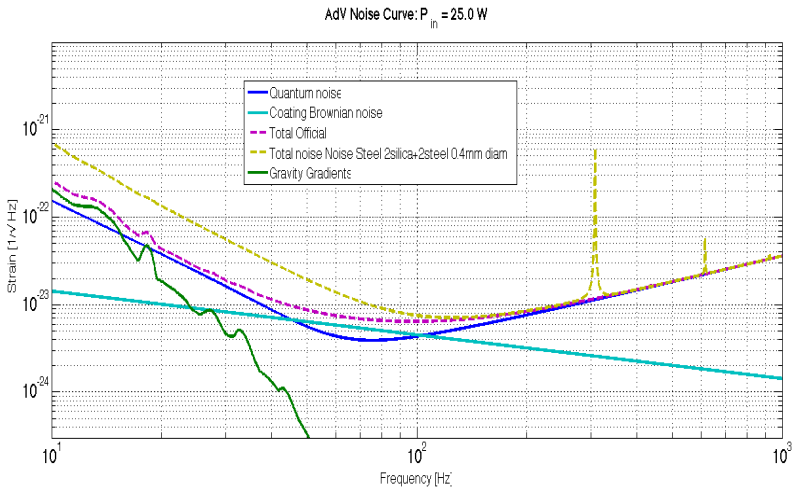

Figure 5: Sensitivity of the case with 2 steel suspensions having diameter of 0.3mm and loss angle of 10^{-4}.

4 Evaluation with the new gwinc version of the case 4 steel suspensions.

	Silica opt	***Steel 400 µm phi=10^{-4} (phi=10^{-3})***	Steel 300 µm phi=10^{-4} (phi=10^{-3})	***Silica 800 µm***
BNS Range (Mpc)	**105**	***45.4 (38)***	60 (51)	***105***
BBH Range (Mpc)	**978**	***202(140)***	313 (199)	***978***

Table 4: Evaluation of the ranges, for 4 payloads, using the new gwinc version used for the computation of the official sensitivities curves. For comparison the VirgoPlus numbers are shown.

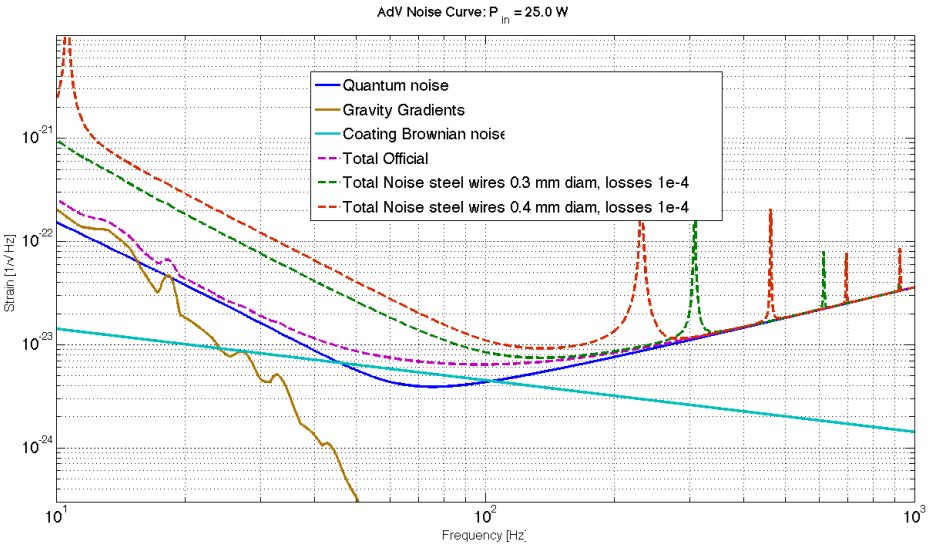

Figure 6: Sensitivity computation in the case of four steel suspensions with 0.3 and 0.4 mm diameter steel wires and 10^{-4} loss angle.

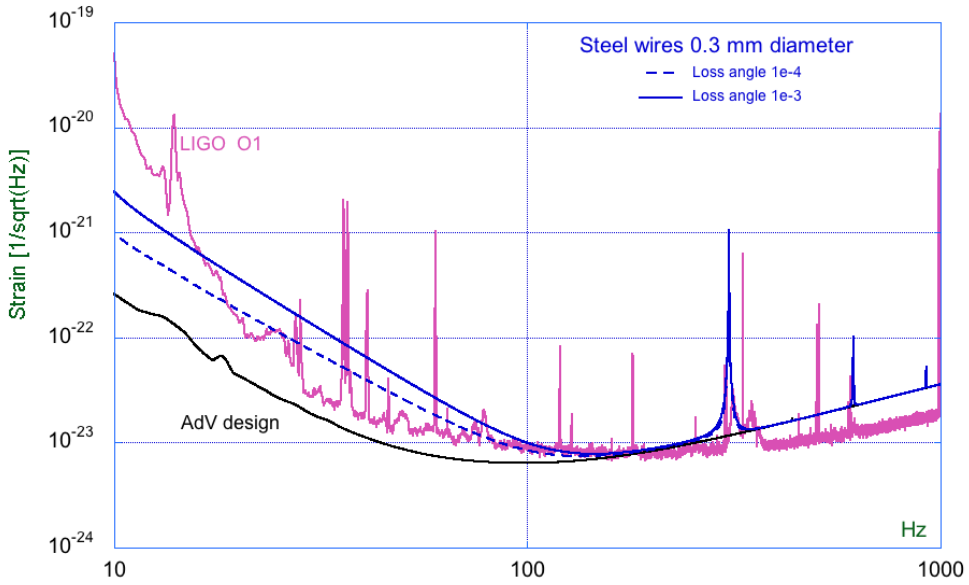

Figure 7: Comparison of the AdV sensitivity curves with the LIGO O1 noise. (phi=1.0e-3 for the steel)

5 Evaluation of the thermal noise using the loss angle measured on the PR mirror steel suspension

The PR mirror is suspended with steel wires with a diameter of 0.3 mm. Recently the quality factor of the first violin mode of this system was measured (logbook entry 34255) and resulted to be $2.28\ 10^5$.

The dilution factor of the violin mode is:

$$D_{viol} = \frac{2}{L_{wire}}\sqrt{\frac{Y_{steel}\ I_o}{\Lambda}} = 3.6\ 10^{-3}$$

where $\Lambda = M_{PR}g/4$ is the wires tension with $M_{PR} = 21\ kg$, $I_o = \pi\ r_w^4/4$ and $r_w = 0.3\ mm$, $Y_{steel} = 200\ GPa$ the Young modulus of the steel, L_{wire}=0.7 m the wire length. Supposing the extra loss in the steel wires is not viscous, we can extrapolate a loss angle of

$$\phi_{steel} = 1.2\ 10^{-3}$$

With the measured value we have estimated the thermal noise and included it in the sensitivity curve. We then calculated the horizons as explained in the paragraph 6.

6 Horizon Computation

The horizon can be computed evaluating the distance at which an optimally oriented binary system, i.e. a system located over the IFO and face-on/face-off, produces an SNR equal to 8. This can be done evaluating numerically the optimal SNR, i.e. the matched-filter of the signal (the template) with itself, using as weight different sensitivity curves corresponding to the configurations:

- 4 mirror suspensions with steel wires of 0.3 mm diameter and loss angle of 10^{-3}
- 4 mirror suspensions with steel wires of 0.3 mm diameter and loss angle of 10^{-4}

Note that the range, i.e. the volume- and orientation-averaged distance at which a compact binary coalescence gives a matched filter signal-to-noise ratio (SNR) of 8, is a factor of 2.26 smaller than the horizon.

We performed these computations using two LAL codes: *lalapps_inspinj* to produce an xml table with all the required characteristics for the template, and *pycbc_optimal_snr* to compute the optimal SNRs for the template in the xml table; the same code then stores the result in selectable columns of the same xml table.
To produce the injection over the IFOs, we choose a GPS time and then identified the declination (latitude) and RA (longitude) of the zenith (the Local Sideral Time). The masses of the bodies in the binary systems were chosen in the detector frame as 1.4 solar masses for a Neutron Star and 30 solar masses for a Black Hole.
The codes with the input parameters used are reported in the appendix.

We also computed the optimal snrs of the two O1 events GW150914 and GW151226 in the different Virgo configurations; in these cases the parameters of the binary systems (GPS, masses, inclination, spins) were taken as the values reported in the LSC-Virgo publications (arXiv 1606.04856, arXiv 1602.03840); for the events location we choose the coordinates of the maximal probability pixel of the most realiable skymaps sent to the observing patners (skymap LALInference and skymap BAYESTAR respectively).
Beware that these snrs are sligthly larger than snrs that can be obtained during a search as they use as templates waveforms that perfectly match the signals.

In table A we report the horizons for the chosen Virgo configurations and in table B the snrs of the O1 events:

Virgo Configuration		BNS HORIZON	BBH HORIZON
AdEarly		236 Mpc	2.5 Gpc
10^{-3}/ 0.3 mm		115 Mpc	1.2 Gpc
10^{-4}/ 0.3 mm		135 Mpc	1.4 Gpc

Table 5

Virgo Configuration		GW150914 snr	GW151226 snr
AdEarly		24	10
10^{-3}/ 0.3 mm		12	4
10^{-4}/ 0.3 mm		14	5

Table 6

7 APPENDIX

Commands used for the BNS horizons:

```
lalapps_inspinj --f-lower 20 --gps-start-time 1467637400 --gps-end-time
1467637564 --time-step 200 --i-distr fixed --fixed-inc 0.0
--l-distr fixed --polarization 80.0 --longitude 134.0 --latitude  43.6311 --
d-distr uniform --min-distance 100000 --max-distance 100000
--m-distr fixMasses --fixed-mass1 1.4 --fixed-mass2 1.4 --disable-spin --
waveform SpinTaylorT4threePointFivePN --taper-injection start
--write-compress --seed 5 --output sim_BNSoverVirgo_f020_100000kpc.xml.gz
```

```
pycbc_optimal_snr -i sim_BNSoverVirgo_f020_100000kpc.xml.gz -o out_BNS-
Adv_early-30Hz-D100000kpc.out --asd-file V1:Adv_early.txt
--f-low 30 --sample-rate 10000 --snr-columns V1:alpha1
```

Commands used for the BBH horizons:

```
lalapps_inspinj --f-lower 20 --gps-start-time 1467637562 --gps-end-time
1467637564 --time-step 100 --i-distr fixed --fixed-inc 180.0
--l-distr fixed --polarization 80.0 --longitude 134.0 --latitude  43.6311 --
d-distr uniform --min-distance 100000 --max-distance 100000
--m-distr fixMasses --fixed-mass1 30 --fixed-mass2 30 --disable-spin --
waveform SEOBNRv2pseudoFourPN --taper-injection start
--write-compress --seed 5 --output sim_BBHoverVirgo_f020_D100000kpc.xml.gz

pycbc_optimal_snr -i sim_BBHoverVirgo_f020_D100000kpc.xml.gz -o out_BBH-
Adv_early-30Hz-D100000kpc.out --asd-file V1:Adv_early.txt
 --f-low 30 --sample-rate 10000 --snr-columns V1:alpha1
```

Note that we computed the optimal snr for a distance of 100 Mpc, and then this distance was rescaled to the value of snr equal to 8.

Commands used for the GW150914 snr computation:

```
lalapps_inspinj --f-lower 10 --gps-start-time 1126259452 --gps-end-time
1126259472 --ipn-gps-time 1126259462.43 --time-step 20
--i-distr fixed --fixed-inc 145.19 --l-distr fixed --polarization 88.84 --
latitude -69.79389 --longitude 134.79545 --d-distr uniform
--min-distance 420000 --max-distance 420000 --m-distr fixMasses --fixed-
mass1 39 --fixed-mass2 31 --enable-spin --aligned
--axis-choice angmomentum --max-spin1 0 --min-spin1 0 --max-spin2 0 --min-
spin2 0 --waveform SEOBNRv2pseudoFourPN --taper-injection start
--write-compress --seed 2 --output sim_from_PEwROMpsdFit-GW150914.xml.gz

pycbc_optimal_snr -i sim_from_PEwROMpsdFit-GW150914.xml.gz -o out_Adv_early-
GW150914-30Hz.out --asd-file V1:Adv_early.txt --f-low 30
--sample-rate 10000 --snr-columns V1:alpha1
```

Commands used for the GW151226 snr computation:

```
lalapps_inspinj --f-lower 10 --gps-start-time 1135136299 --gps-end-time
1135136351 --ipn-gps-time 1135136324 --time-step 100 --i-distr fixed
--fixed-inc 0 --l-distr fixed --polarization 0 --latitude 34.22887 --
longitude 52.55859 --d-distr uniform --min-distance 440000
--max-distance 440000 --m-distr fixMasses --fixed-mass1 15.8 --fixed-mass2
8.2 --enable-spin --aligned --axis-choice angmomentum
--max-spin1 0.2 --min-spin1 0.2 --max-spin2 0 --min-spin2 0 --waveform
SEOBNRv2pseudoFourPN --taper-injection start --write-compress
--seed 2 --output sim_from_PEwROMpsdFit-GW151226.xml.gz

pycbc_optimal_snr -i sim_from_PEwROMpsdFit-GW151226.xml.gz -o out_Adv_early-
30Hz-GW151226.out --asd-file V1:Adv_early.txt --f-low 30
--sample-rate 10000 --snr-columns V1:alpha1
```

Note that for GW150914 and GW151226 snrs computation we have used the detector frame masses, which are a factor of (1 + z) larger than the source frame masses.